RESEARCH ARTICLE | SEPTEMBER 17 2020

Spin dynamics in experiments on orthodeuterium induced polarization (ODIP)

Vitaly P. Kozinenko; Alexey S. Kiryutin ; Stephan Knecht; Gerd Buntkowsky ; Hans-Martin Vieth ; Alexandra V. Yurkovskaya ; Konstantin L. Ivanov

J. Chem. Phys. 153, 114202 (2020)
https://doi.org/10.1063/5.0022042

The Journal of Chemical Physics ARTICLE scitation.org/journal/jcp

Spin dynamics in experiments on orthodeuterium induced polarization (ODIP)

Cite as: J. Chem. Phys. 153, 114202 (2020); doi: 10.1063/5.0022042
Submitted: 16 July 2020 • Accepted: 19 August 2020 •
Published Online: 17 September 2020

Vitaly P. Kozinenko,[1,2] Alexey S. Kiryutin,[1,2] Stephan Knecht,[3] Gerd Buntkowsky,[3] Hans-Martin Vieth,[1,4] Alexandra V. Yurkovskaya,[1,2] and Konstantin L. Ivanov[1,2,a)]

AFFILIATIONS

[1] International Tomography Center, Siberian Branch of the Russian Academy of Science, Novosibirsk 630090, Russia
[2] Novosibirsk State University, Novosibirsk 630090, Russia
[3] Eduard-Zintl Institute for Inorganic and Physical Chemistry, TU Darmstadt, Darmstadt 64287, Germany
[4] Institut für Experimentalphysik, Freie Universität Berlin, Berlin 14195, Germany

[a)] **Author to whom correspondence should be addressed:** ivanov@tomo.nsc.ru

ABSTRACT

A comprehensive description of the spin dynamics underlying the formation of *Ortho*-Deuterium Induced Polarization (ODIP) is presented. ODIP can serve as a tool for enhancing Nuclear Magnetic Resonance (NMR) signals of ^{2}H nuclei, being important probes of molecular structure and dynamics. To produce ODIP, in the first step, the D_2 gas is brought to thermal equilibrium at low temperature, here 30 K, so that the *ortho*-component, corresponding to the total spin of the ^{2}H nuclei equal to 0 and 2, is enriched, here to 92%. In the second step, the orthodeuterium molecule is attached to a substrate molecule using a suitable hydrogenation catalyst such that the symmetry of the two ^{2}H nuclei is broken. As a result, the non-thermal spin order of orthodeuterium is converted into enhancement of observable NMR signals. In this work, we perform a theoretical study of ODIP and calculate the shape of ODIP spectra and their dependence on the magnetization flip angle. These results are compared with experiments performed for a number of substrates; good agreement between experimental and calculated ODIP spectra is found. We also discuss the performance of NMR techniques for converting anti-phase ODIP spectral patterns into in-phase patterns, which are more suitable for signal detection and for transferring ODIP to heteronuclei, here to ^{13}C spins. Experimental procedures reported here allowed us to reach signal enhancement factors of more than 1000 for ^{2}H nuclei in the liquid phase. These results are useful for extending the scope of spin hyperpolarization to the widely used ^{2}H nuclei.

I. INTRODUCTION

Spin hyperpolarization offers powerful methods for enhancing weak NMR (Nuclear Magnetic Resonance) signals by using spin systems that are far off-thermal equilibrium. Generally, the NMR signal intensity for a transition $|i\rangle \rightarrow |f\rangle$ is directly proportional to the population difference, $(P_i - P_f)$, between the corresponding states, which is very small under equilibrium conditions. For a hyperpolarized spin system, this difference can be dramatically increased giving rise to strong signal enhancement. One of the widely used hyperpolarization techniques is *Para*-Hydrogen Induced Polarization (PHIP),[1–3] which makes use of the spin order of parahydrogen (pH$_2$, the H_2 molecule in its nuclear singlet spin state). Parahydrogen and orthohydrogen (oH$_2$, the H_2 molecule in its nuclear triplet spin state) are termed "spin isomers" of H_2. In the H_2 molecule in the gas phase, the nuclear spin degrees of freedom are coupled to rotational states due to the symmetry of the total wavefunction with respect to exchanging the two protons. Hence, since the rotational quantum is approximately equal to 175 K, pH$_2$ is relatively easy to prepare by equilibrating the H_2 gas at a low temperature: at 77 K, the population of the *para*-component of H_2 is as large as 50% instead of 25% at high temperature; slightly above the H_2 freezing point, almost 100% of pH$_2$ is expected. This overpopulation of the singlet state (spin order) of pH$_2$ can be efficiently converted into NMR signal enhancement by using chemical reactions, which break the symmetry of the two protons of the NMR-silent pH$_2$. In practice, this is done

by catalytic hydrogenation reactions[2,4] or by polarization transfer in a transient complex, which binds pH$_2$ and a to-be-polarized substrate.[5,6]

H$_2$ is not the only diatomic molecule in which specific spin isomers can be enriched. One should note, however, that the rotational energy is inversely proportional to the moment of inertia of the molecule, i.e., to its mass. For this reason, the straightforward enrichment method by equilibrating the gas at a low temperature meets difficulties for heavier molecules. In practice, only orthodeuterium (oD$_2$) is relatively easy to prepare: for instance, at 77 K, one expects 71% of oD$_2$ instead of 66.7% at room temperature. At 30 K, the temperature used in this work, the oD$_2$ content is higher, reaching 92%. By using oD$_2$, as shown by Bargon and co-workers,[7] one can also obtain enhanced NMR signals and thus generate *Ortho*-Deuterium Induced Polarization (ODIP). We would like to note that the term "ODIP" does not exactly reflect the underlying physics, since the state of a spin-1 nucleus (being a three-level quantum system) is not completely characterized in terms of spin polarization. Nonetheless, we use this term, which is accepted by the community. After this demonstration of ODIP feasibility, the number of publications about ODIP has been very limited: more information about this method can be found only in the PhD theses by Limbacher[8] and Jonischkeit.[9] However, one should note that ODIP has the potential of a powerful hyperpolarization method, as it allows one to hyperpolarize D-nuclei, which are widely used in NMR studies. Efficient hyperpolarization of D-nuclei in the liquid state is generally challenging because of fast quadrupolar relaxation and is so far limited to only a few examples of experiments using ODIP (mentioned above), dissolution dynamic nuclear polarization,[10–12] and polarization transfer from neighboring heteronuclei.[13]

In this work, we perform a systematic study of ODIP aiming on the one hand at a deep theoretical understanding of the underlying spin dynamics, overcoming experimental hurdles and formulating practical recommendations on how to perform ODIP experiments. We start with a theoretical description of ODIP and then proceed to experimental implementation and optimization of the technique. In our experiments, we work with several substrates and perform experiments at elevated temperature and bubbling pressure in order to maximize ^{2}H NMR enhancement. On the other hand, we study how ODIP depends on the strength of the magnetic field at which the chemical reaction of hydrogenation with oD$_2$ is performed. Last but not least, we propose methods for converting anti-phase ODIP signals into in-phase signals in order to avoid signal cancellation and perform high-field polarization transfer to ^{13}C nuclei.

II. METHODS

A. Theoretical description of ODIP

Here, we start with a theoretical treatment of ODIP to fill some gaps in existing spin dynamics simulations. Previously, the shape of NMR spectral patterns has been considered in detail for the case where polarization is generated at a high magnetic field B_0; at the same field, the NMR spectrum is taken. This case corresponds to the PASADENA (parahydrogen and synthesis allow dramatically enhanced nuclear alignment) experiment.[4] In this case, the shape of the spectra patterns has been derived as well as the dependence of the signal intensity on the magnetization flip angle φ used in a pulse NMR experiment. As usual, the flip angle is defined as $\varphi = \omega_1\tau_p = \gamma B_1\tau_p$, where B_1 is the strength of the RF-field, γ is the gyromagnetic ratio, and τ_p is the pulse duration. However, other pulse experiments have not been considered. In this work, we also treat a spin-echo experiment performed under the PASADENA conditions.

A more complex situation arises when the hydrogenation reaction, which gives rise to ODIP, is performed at a low field B_{pol}, and subsequently, the sample is transferred to the high field B_0 of an NMR spectrometer. This experimental protocol is commonly termed ALTADENA (Adiabatic Longitudinal Transport After Dissociation Engenders Net Alignment).[14] In this situation, the state populations at the detection field have been calculated,[8] assuming the limiting case of ideal adiabatic transfer of the sample to the measurement field. For this population pattern, the shape of the continuous-wave NMR spectrum has been derived. One should note, however, that in pulsed experiments, the spectral pattern strongly depends on φ and that only the spectrum at $\varphi \to 0$ has the same shape as the continuous-wave spectrum. So far, the φ-dependence of the spectrum has not been analyzed. Possible effects of the non-adiabatic field variation have also not been considered so far, although in some cases, the spectral pattern significantly deviates from that expected for ideal adiabatic $B_{pol} \to B_0$ field switching. The situation is further complicated by the presence of additional nuclei in the hyperpolarized substrate molecules, which affect the polarization pattern. In this work, we consider the effects of non-adiabatic field switching and the influence of additional nuclei.

Altogether, there are nine spin states of the D$_2$ molecule, which correspond to the states with total spin equal to 0 (singlet), 1 (triplet), and 2 (quintet). These states are introduced in Appendix A. When the oD$_2$ isomer is fully enriched, only the singlet state $|S\rangle$ and five quintet states $|Q_i\rangle$ are populated. Hence, the density matrix of oD$_2$ is as follows:

$$\rho = \hat{\rho}_{ortho} = |S\rangle\langle S| + \sum_{i=-2}^{2} |Q_i\rangle\langle Q_i|. \tag{1}$$

To treat the spin dynamics, it is convenient to introduce the spin density matrix in the operator basis. In this representation, the expression for $\hat{\rho}_{ortho}$ is as follows:

$$\hat{\rho}_{ortho} = \frac{2}{3}\hat{E} + \frac{1}{4}\left(\hat{I}_{1z}\hat{I}_{2z} + \hat{I}_{1x}\hat{I}_{2x} + \hat{I}_{1y}\hat{I}_{2y} + \hat{I}_{1a}\hat{I}_{2a} + \hat{I}_{1b}\hat{I}_{2b} + \hat{I}_{1c}\hat{I}_{2c} + \hat{I}_{1d}\hat{I}_{2d} + \hat{I}_{1e}\hat{I}_{2e}\right). \tag{2}$$

The basis operators are also introduced in Appendix A. Upon rotation of spins, the x, y, z operators are transformed in the same way as those for spin-1/2, whereas the a, b, c, d, e operators are transformed in a more complex way (similar to the components of the quadrupolar tensor, i.e., of a symmetric traceless tensor).[15] The Hamiltonian of the spin system under study placed at the external field B is written in the usual way (in h units),

$$\widehat{\mathcal{H}}(B) = -\nu_1\hat{I}_{1z} - \nu_2\hat{I}_{2z} + J_{12}\left(\hat{I}_{1z}\hat{I}_{2z} + \hat{I}_{1x}\hat{I}_{2x} + \hat{I}_{1y}\hat{I}_{2y}\right). \tag{3}$$

Here, $\nu_i = (1 + \delta_i)\gamma B/2\pi$ is the Zeeman interaction of the ith spin given by its chemical shift δ_i, while J_{12} is the scalar spin–spin

coupling between the spins. When necessary, the spin system can be extended to more than two coupled spins. To do so, one should take the direct product of $\hat{\rho}_{ortho}$ and the equilibrium density matrix of other spins, $\hat{\rho}_{eq}$, to compose the total density matrix and consider additional Zeeman interactions and J-couplings in the Hamiltonian. One should note that the coupling term in Eq. (3) may contain additional contributions coming from exchange properties of the wave-function of the two equivalent D-nuclei.[16] However, here, we refrain from discussing the role of these terms, which are irrelevant at high magnetic fields.

1. PASADENA experiment

In the PASADENA case, it is sufficient to consider only the two D-spins because at a high field, other spins in the molecule, e.g., protons, are "weakly coupled" to the polarized D-spins, meaning that there is no polarization transfer to these spins. Consequently, interactions with these spins only give rise to additional splitting of NMR multiplets, but not to extra polarization features.

When considering the spin dynamics, one should note that chemical reactions that give rise to ODIP typically last for several seconds. In this situation, different polarized molecules are formed at different instants of time. Consequently, spin coherences generated by ODIP are efficiently washed out because these coherences start with random phases and disappear after ensemble averaging.[17,18] The coherent terms in Eq. (2) are all terms except for $\hat{I}_{1z}\hat{I}_{2z}$ and $\hat{I}_{1a}\hat{I}_{2a}$; hence, the density matrix changes as follows:

$$\hat{\rho}_{ortho} \rightarrow \hat{\rho}_P = \frac{2}{3}\hat{E} + \frac{1}{4}\left(\hat{I}_{1z}\hat{I}_{2z} + \hat{I}_{1a}\hat{I}_{2a}\right). \tag{4}$$

Here, the unity operator does not reveal itself in NMR experiments and can be omitted as well. Upon rotations of spins, the operators of interest are transformed as follows:[7]

$$\hat{I}_{1z}\hat{I}_{2z} \xrightarrow{\varphi\hat{I}_x} \cos^2\varphi\hat{I}_{1z}\hat{I}_{2z} + \sin^2\varphi\hat{I}_{1y}\hat{I}_{2y} + \cos\varphi\sin\varphi\left(\hat{I}_{1z}\hat{I}_{2y} + \hat{I}_{1y}\hat{I}_{2z}\right) \tag{5}$$

and

$$\hat{I}_a \xrightarrow{\varphi\hat{I}_x} 3\left(\cos^2\varphi - 1\right)\hat{I}_a + \left(\sqrt{\frac{3}{2}}\sin 2\varphi\right)\hat{I}_c + \left(\frac{\sqrt{3}}{2}\sin^2\varphi\right)\hat{I}_e. \tag{6}$$

Hence, rotation of $\hat{I}_{1a}\hat{I}_{2a}$ gives rise to nine different operators. Here, we consider rotations about the x-axis of the rotating frame, thus assuming that RF-pulses have x-phase. After application of the RF-pulse, different terms in the density matrix start evolving under the action of the Hamiltonian $\widehat{\mathcal{H}}(B = B_0)$. When considering this evolution, it is sufficient to consider only the part, which gives rise to observable magnetization given by $\hat{I}_x = \hat{I}_{1x} + \hat{I}_{2x}$ and $\hat{I}_y = \hat{I}_{1y} + \hat{I}_{2y}$. The only terms that thus become important are the $\hat{I}_{1z}\hat{I}_{2y}$ and $\hat{I}_{1y}\hat{I}_{2z}$ terms. Hence, we immediately obtain that the signal intensity is directly proportional to $\sin 2\varphi$ being optimal at $\varphi = \pi/4$ and zero at $\varphi = \pi/2$.

To simulate NMR spectra, we used the same procedure as before.[17,19] We introduce the density matrix, which is obtained after the action of an RF-pulse on $\hat{\rho}_P$,

$$\hat{\rho}' = \exp\left[-i\varphi\hat{I}_x\right]\hat{\rho}_P\exp\left[i\varphi\hat{I}_x\right], \tag{7}$$

and write this density matrix using the $\hat{I}_+ = \hat{I}_x + i\hat{I}_y$ operator in the eigen-basis of $\widehat{\mathcal{H}}(B = B_0)$. After that, the Fourier-transform NMR spectrum can be evaluated as follows:[20]

$$S(\nu) \sim \frac{\sum_{i,j}\left(\hat{I}_+\right)_{ij}\hat{\rho}'_{ij}}{2\pi i\delta\nu_{ij} + 1/T_2}. \tag{8}$$

Here, $S(\nu)$ is the NMR intensity at the frequency ν, with $\delta\nu_{ij} = \nu_{ij} - \nu$ and $\nu_{ij} = E_i - E_j$ [$E_{i,j}$ are the eigen-values of $\widehat{\mathcal{H}}(B_0)$]; T_2 determines the characteristic NMR linewidth.

PASADENA spectra for a two-spin system are shown in Fig. 1. One can see that in each NMR multiplet, only two lines out of three have non-zero intensity; hence, each multiplet looks like an anti-phase doublet. The line intensity is proportional to $\sin 2\varphi$.

Using the same calculation method, we can also evaluate the effect of pulse sequences on the hyperpolarized spin system. For instance, if we apply the spin echo sequence φ_x-delay–π_x-delay at $t = 2\tau$ (here, τ is the delay), spin magnetization is refocused, i.e., an echo signal is formed. Interestingly, in the case of anti-phase polarization given by the $\hat{I}_{1z}\hat{I}_{2z}$ term (as in the previous case, the term $\hat{I}_{1a}\hat{I}_{2a}$ does not contribute to the signal), "out-of-phase" spin magnetization is collected,[21] corresponding to $\hat{I}_x$ but not to $\hat{I}_y$ operator. The echo signal is as follows:

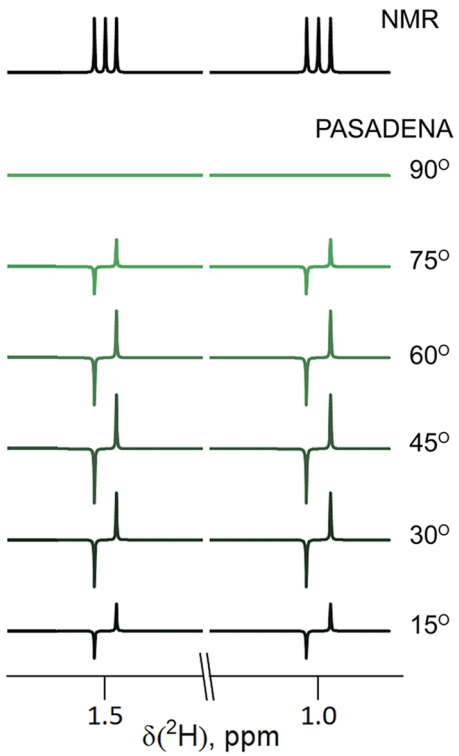

FIG. 1. Calculated ODIP spectra obtained for the PASADENA experiment for different magnetization flip angles of the detecting pulses. Calculation parameters: δ_1 = 1 ppm, δ_2 = 1.5 ppm, and J = 1 Hz.

$$\hat{I}_x(2\tau) = \frac{1}{2}\sin 2\varphi \sin(4\pi J\tau)\hat{I}_{1z}\hat{I}_{2z}. \quad (9)$$

Hence, the echo amplitude is maximal at $\varphi = \pi/4$ and $\tau = 1/8J$. The advantage of the out-of-phase signal detection is that this signal does not contain contributions from thermal polarization, which is refocused in the in-phase channel. Hence, this method provides efficient suppression of unwanted thermal signals in the spectrum.[21]

2. ALTADENA experiment

In the ALTADENA case, first, the low-field eigen-states are populated: these states are the singlet and quintet states $|J, M_J\rangle$ with $J = 0, 2$ and $M_J = -J, \ldots, J$. Hence, at low B_{pol}, six spin states out of nine will acquire identical populations. When the sample is transported to B_0 in an adiabatic fashion, one should correlate the low-field and high-field states, as has been done before.[19] Hence, six high-field states will be populated, and these states are $|\alpha\alpha\rangle$, $|\beta\alpha\rangle$, $|\beta\beta\rangle$, $|\gamma\alpha\rangle$, $|\gamma\beta\rangle$, and $|\gamma\gamma\rangle$, where $|\alpha\rangle$, $|\beta\rangle$, and $|\gamma\rangle$ indicate that M_J equal −1, 0, and 1, respectively. The resulting density matrix is then given as follows (see discussion in Appendix B):

$$\hat{\rho}_A = \frac{2}{3}\hat{E} + \frac{1}{6}\left[\hat{I}_{1z} - \hat{I}_{2z} + \sqrt{3}\left(\hat{I}_{1a}\hat{I}_{2z} - \hat{I}_{1z}\hat{I}_{2a}\right) + \sqrt{3}\left(\hat{I}_{1a} + \hat{I}_{2a}\right)\right]. \quad (10)$$

The NMR pattern in this case becomes rather complex (see Fig. 2). One can see that in each multiplet, the integrated intensity of all three lines is non-zero; at the same time, the central line and the outer lines behave differently as the flip angle is varied. Specifically, the flip angle dependence of the central line is given by $\{\sin\varphi + \sin 3\varphi\}$; for the outer line it is $\frac{1}{2}\{3\sin\varphi - \sin 3\varphi\}$. Hence, at small φ, the outer lines have negligibly small intensities, and at $\varphi = \pi/4$, we obtain 1:2:1 intensity ratio in the multiplets, while at $\varphi = \pi/2$, the central lines disappear (see Fig. 2). It is useful to note that the total intensity of each multiplet, which is proportional to $\sin\varphi$, has a maximum at flip angle $\varphi = \pi/2$: this is helpful for optimizing the enhancement in the case when the splitting in NMR multiplets is not resolved. When the sign of J is negative, the sign of polarization is inverted, as shown in Appendix B. One should note, however, that ALTADENA experiments imply that field variation is adiabatic, which is not always the case, as discussed below. When the adiabaticity condition is not fulfilled, it is more appropriate to term such experiments *ODIP experiments with polarization at low field*.

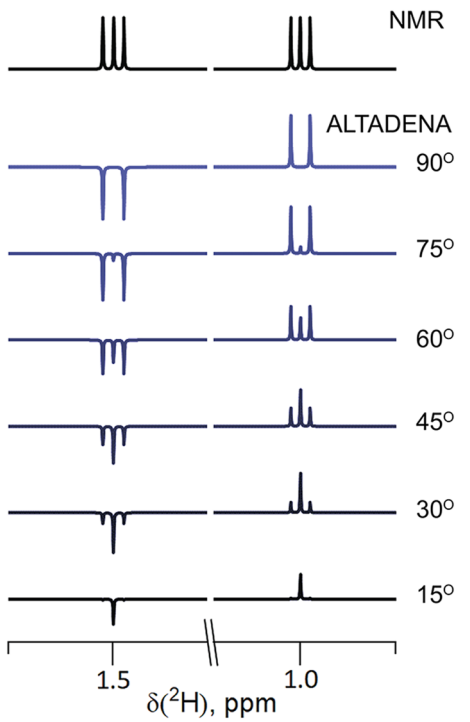

FIG. 2. Calculated ODIP spectra obtained for the ALTADENA experiment at different magnetization flip angles of the detecting pulses. Calculation parameters: $\delta_1 = 1$ ppm, $\delta_2 = 1.5$ ppm, and $J = 1$ Hz.

3. Numerical calculations

Some of the calculations performed in this work have been done only numerically. This has been done, for instance, to describe spin evolution upon field variation $B_{pol} \to B_0$ using realistic $B(t)$ time profiles and to elucidate the role of a third spin in the molecules, here, of an additional proton. To perform such calculations, we proceed as follows:[17,19] First, the initial density matrix

$$\hat{\rho}_0 = \hat{\rho}_{ortho} \otimes \hat{\rho}_{eq} \quad (11)$$

is calculated in the eigen-basis of the Hamiltonian $\widehat{\mathcal{H}}\left(B = B_{pol}\right)$. Here, $\hat{\rho}_{eq}$ is the density matrix of thermally polarized spins. In the case of an additional proton, this matrix is a 2×2 matrix with two non-zero diagonal elements, which are equal to $\frac{1}{2}$ if we neglect the small thermal polarization. Due to the finite preparation period, all off-diagonal elements of $\hat{\rho}_0$ can be set equal to zero [only when this matrix is written in the eigen-basis of $\widehat{\mathcal{H}}\left(B = B_{pol}\right)$]. Subsequently, the time evolution can be computed by splitting the time interval into many small steps of the duration δt, assuming that the Hamiltonian is almost constant within each step and evaluating the density matrix at the $(n+1)$-th step by relating it to that at the previous step as follows:

$$\hat{\rho}_{n+1} = \exp\left[-2\pi i\widehat{\mathcal{H}}_n\delta t\right]\hat{\rho}_n \exp\left[2\pi i\widehat{\mathcal{H}}_n\delta t\right]. \quad (12)$$

In this way, the density matrix after the field switching can be calculated at $B = B_0$; after that, the NMR spectrum can be obtained in the same way as described above.

B. Materials and reactions

To enrich the D_2 gas with its *ortho*-component, we used a commercial closed-cycle cryocooler DE-204 from "Advanced Research Systems, Inc." Cooling the D_2 gas down to 30 K being slightly above the boiling point allowed us to achieve a concentration of the *ortho*-component equal to 92%.

The basic principles of creating ODIP in the course of hydrogenation with oD_2 are the same as those in the case of PHIP. Therefore, as a starting point in all optimizations of ODIP

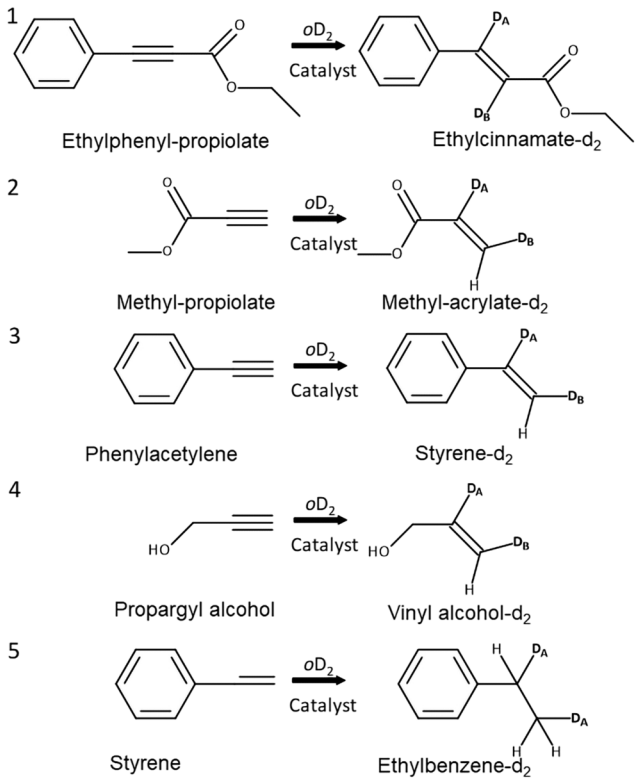

SCHEME 1. Schemes of chemical reactions, here, hydrogenation by oD_2, used in this work to generate ODIP.

experiments, we used the reaction conditions, known to be working best in experiments with pH_2. For running ODIP experiments, we used the following substrates having a double or triple C–C bond: methylpropiolate, phenylacetylene, ethyl-phenylpropiolate, styrene, and propargyl alcohol. PHIP experiments with these compounds demonstrate high signal enhancements, which makes them a good model for ODIP optimization.[17,22] All substances were purchased from Sigma-Aldrich and used without further purification. After hydrogenation of these products, we obtain products with two hyperpolarized D-nuclei, indicated as D_A and D_B. The schemes of the corresponding hydrogenation reactions are shown in Scheme 1 as well. To run NMR experiments, we used a 5 mm NMR tube filled with 600 μl of methanol-d_4 used as a solvent with 40 mM of the substrate and 5 mM of the catalyst, 1,4-Bis(diphenylphosphino)butane(1,5-cyclooctadiene)Rh(I) tetrafluoroborate (from Sigma-Aldrich). Table I presents the T_1-relaxation times of the D_A and D_B nuclei in the compounds that we used and enhancement factors, ε, achieved in ODIP experiments, performed under PASADENA and ALTADENA conditions. For calculation of the ODIP enhancement factors, the area under the lines of hyperpolarized signals in its magnitude was integrated and compared to the integrated intensity of the corresponding thermal signals. Since individual lines in NMR multiplets strongly overlap with each other, we present an average enhancement factors for the multiplets of D-nuclei instead of giving enhancements for each single line. NMR parameters of the molecules under study are discussed in Appendix C.

C. NMR experiments

All NMR spectra were obtained with a BRUKER AVANCE II console and an Oxford 500 MHz NMR magnet (the magnetic field at the detection zone was 11.7 T). For the ^{2}H nuclei, the Larmor frequency at this magnetic field is equal to 76.9 MHz. We performed NMR experiments according to the protocols depicted in Fig. 3. In all cases, we start with D_2 gas enriched in its oD_2 component and bubble it through the sample in order to initiate the hydrogenation reactions, which give rise to ODIP, using the *in situ* gas supply system described before.[23] The available system allows bubbling gas through the sample placed inside an NMR probe under variable pressure. The system is also compatible with NMR experiments using magnetic field variation. A major task in ODIP is maximizing the polarization rate because of the fast quadrupolar relaxation of ^{2}H. Thus, efforts were taken to speed up the hydrogenation reaction and minimize duration of all steps before signal acquisition.

TABLE I. T_1 relaxation of deuterium nuclei D_A and D_B in reaction products and corresponding enhancements ε in PASADENA and ALTADENA 90 (ALTADENA detection with $\frac{\pi}{2}$ pulse) experiments at 50 °C.

Product molecule	Nucleus	T_1 (s)	ε		
			PASADENA	ALTADENA 90	Out-of-phase echo
Ethyl-cinnamate-d_2	D_A	0.38	78	60	...
	D_B	0.31	77	60	...
Methyl-acrylate-d_2	D_A	1.01	630	1350	490
	D_B	0.53	685	44	470
Styrene-d_2	D_A	1.06	301	...	...
	D_B	0.56	309	...	...
Vinyl-alcohol-d_2	D_A	1.28	682	...	...
	D_B	1.03	1080	...	...
Ethylbenzene-d_2	D_A	1.82	30	...	...
	D_B	1.29	34	...	...

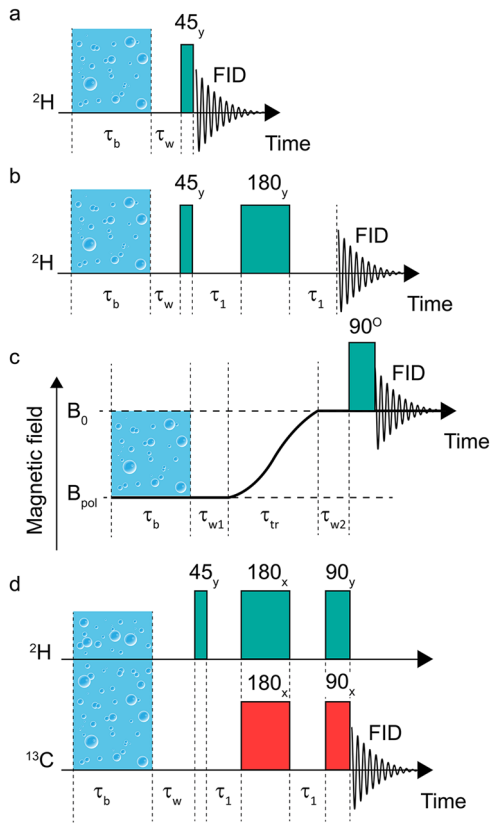

FIG. 3. Timing schemes of the ODIP experiments performed in this study. Protocol (a) PASADENA experiment in which the D_2 gas enriched in the *ortho*-component is bubbled through the solvent during a time period τ_b; after the waiting period of a duration τ_w, the NMR spectrum is acquired after applying an RF pulse (typically, a $\frac{\pi}{4}$-pulse is used). Protocol (b) out-of-phase echo experiment in which after the bubbling and waiting periods, the echo sequence is applied (with the flip angle of the first pulse being equal to $\frac{\pi}{4}$) and the out-of-phase component of the FID signal is detected; the first FID point is taken at the instant of time when magnetization is refocused. Protocol (c) ALTADENA experiment in which gas bubbling is performed at a low B_{pol} field, where the D-nuclei are strongly coupled; subsequently, after a short delay τ_{w1}, the sample is transported during τ_{tr} to the B_0 field where the NMR spectrum is taken. Delay τ_{w2} before spectrum acquisition allows one to minimize signal distortions caused by the finite settling time of observation field B_0. Protocol (d) PH-INEPT pulse sequence used to enhance the signals of ^{13}C nuclei by coherent transfer of ODIP.

Increasing the rate of hydrogenation reaction by sample heating or bubbling at elevated pressure gives a straightforward way of maximizing the enhancements in both PHIP and ODIP experiments. However, in the case of hydrogenation with oD$_2$, speeding up the reaction is crucial, because of the short relaxation times of D-nuclei in the product molecule and probably an isotope effect of deuterons, which slows down the reaction. We tested the effect of temperature, bubbling pressure, and oD$_2$ enrichment on the level of ODIP enhancement in the PASADENA case (see Table II). These results demonstrate the importance of the proper choice of the reaction conditions in ODIP experiments. All hyperpolarized spectra presented below have been obtained using optimal parameters, i.e., the sample temperature of 50 °C, bubbling pressure of 5 bars, and oD$_2$ enrichment of 92%. Bubbling at 5 bars pressure allows one to achieve D_2 saturation in the sample within 10 s of bubbling. However, this duration of bubbling is not optimal, as the deuterons in the product molecules have T_1 relaxation times of about 1 s. Thus, the duration of the bubbling period, τ_b, was set to 6 s. In the PASADENA experiment, bubbling is performed at the B_0 field, and after a delay τ_w (typically, 0.5 s, required to get rid of gas bubbles, which disturb the homogeneity of the magnetic field across the sample and thus decrease spectral resolution), the Free Induction Decay (FID) signal is measured after applying an RF pulse. Fourier transform of the FID yields the NMR spectrum. Typically, the magnetization flip angle in PASADENA experiments was taken equal to $\pi/4$.

We also updated known protocols for converting the anti-phase polarization, which leads to signal cancellation, into net polarization for high-field ODIP experiments. To do so, we exploit the out-of-phase echo[21] protocol (see Fig. 3). In the echo experiment, we apply two pulses, a $\pi/4$ pulse and a π pulse after delay τ_1, and start detecting the out-of-phase component of the FID signal after another delay τ_1 following the second pulse.

To extend the scope of ODIP experiments to low B_{pol} fields, we also performed experiments with field variation analogous to the ALTADENA protocol. In such experiments, hydrogenation reactions are run at a low magnetic field; subsequently, the field is increased to $B = B_0$ and the FID signal is measured after applying a detection pulse (see Fig. 3). The total time of sample transfer from low field to the spectrometer detection zone was equal to 0.73 s. Waiting delays before (required to get rid of bubbles) and after (required to stabilize at the observation field) sample transfer were set to $\tau_{w1} = 0.03$ s and $\tau_{w2} = 0.25$ s, respectively.

To demonstrate the possibility of ODIP transfer to heteronuclei, we implemented a conventional PH-INEPT experiment[24] (see

TABLE II. ODIP PASADENA signal enhancement of D_A nucleus in the methylacrylate-d_2 molecule obtained at various sample temperatures, gas bubbling pressures, and oD$_2$ enrichments. 71% *ortho* enrichment was obtained by passing the D_2 gas through a spiral copper tube plunged into liquid nitrogen (conversion temperature—77 K).

	oD$_2$ concentration—71%, bubbling pressure—3 bars		oD$_2$ concentration—92%, bubbling pressure—5 bars	
	T = 25 °C	T = 40 °C	T = 25 °C	T = 50 °C
PASADENA ε	10	20	41	630

Fig. 3). This pulse sequence allows us to transform the non-equilibrium multiplet polarization of deuterons into an anti-phase magnetization of the heteronucleus. The optimization of the delay in the refocusing spin echo block requires the knowledge of the J-coupling constant between two deuterons and heteronucleus.

III. RESULTS AND DISCUSSION

A. PASADENA experiments

We performed PASADENA experiments for all ODIP substrates listed in Scheme 1. Experiments were carried out at an elevated temperature of 50 °C and at a bubbling pressure of 5 bars in order to speed up the hydrogenation reactions and hence polarization formation. These results are presented in Figs. 4–8.

For ethylcinnamate-d_2, in the discussed conditions, we managed to obtain enhancement equal to $\varepsilon = 78$ (D_A nucleus) and $\varepsilon = 77$ (D_B nucleus). The observed spectral pattern was modeled theoretically: the simulation is in good agreement with the experimental data (see Fig. 4). The spectral pattern consists of two anti-phase multiplets, in accordance with the results shown in Sec. II A.

A stronger signal enhancement, ε, has been achieved for methylacrylate-d_2, which is $\varepsilon = 630$ (D_A nucleus) and $\varepsilon = 685$ (D_B nucleus) (see Fig. 5). As in the previous case, the experimental spectrum is in good agreement with the spectral pattern predicted by calculation: anti-phase polarization of the two D-nuclei is clearly visible and the NMR lines of H_A are split due to the interaction with the proton. T_1 relaxation of D_B in methylacrylate-d_2 is faster than relaxation of D_A (Table I), yet the signal enhancement for this nucleus is higher, which we attribute to the effect of stronger line cancellation

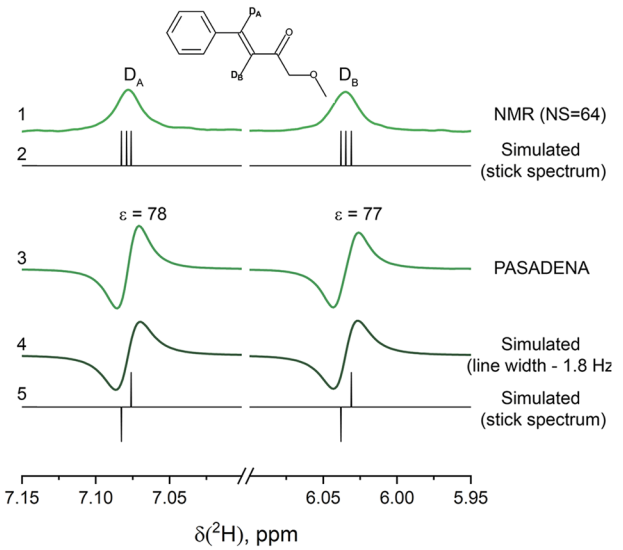

FIG. 4. ^{2}H NMR spectrum of ethyl-cinnamate-d_2 obtained at thermal polarization (1) and with signal enhancement provided by ODIP (3). Experiment is performed under PASADENA conditions at a sample temperature of 50 °C. Numerical simulation of the thermal NMR spectrum is presented as a stick-spectrum (2) and simulation of the ODIP spectrum is presented with 1.1 Hz line broadening (4) and as a stick-spectrum without line broadening (5).

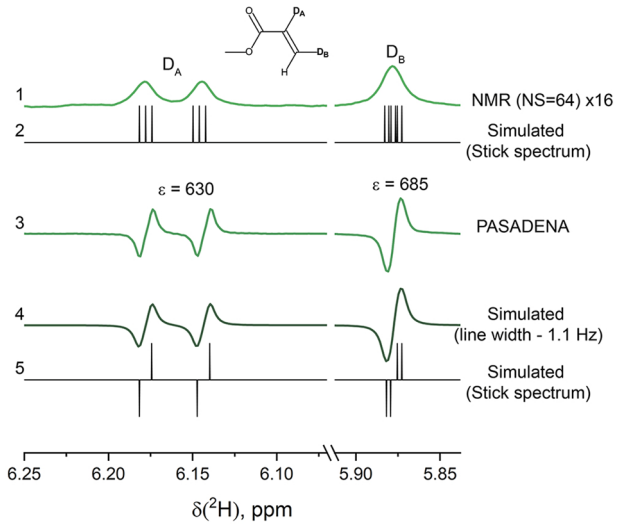

FIG. 5. ^{2}H NMR spectrum of methylacrylate-d_2 obtained with thermal polarization (1) and with signal enhancement provided by ODIP (3). Experiment is performed under PASADENA conditions at a sample temperature of 50 °C. Numerical simulation of the thermal NMR spectrum is shown as a stick-spectrum (2) and simulation of the ODIP spectrum is done with 1.1 Hz line width (4) and as a stick-spectrum (5).

in the D_A multiplet in the ODIP spectrum. An almost ten-fold difference in the signal amplification as compared to ethylcinnamate-d_2 is most likely due to slower relaxation of deuterons in methylacrylate-d_2. The bigger size of ethylcinnamate-d_2 leads to increasing gradients of the electric field over the molecule, which boost the rates of quadrupolar relaxation of deuterons. Another difference with respect to ethylcinnamate-d_2 is the additional line splitting in

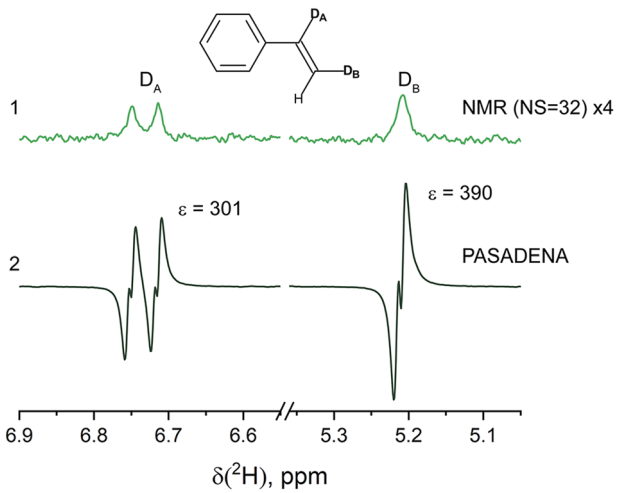

FIG. 6. ^{2}H NMR spectrum of styrene-d_2 obtained using thermal polarization and with signal enhancement provided by ODIP. Experiment is performed under PASADENA conditions at a sample temperature of 50 °C.

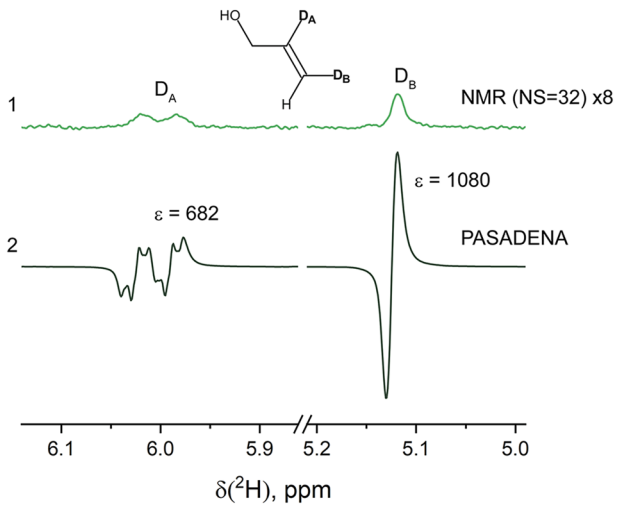

FIG. 7. ^{2}H NMR spectrum of vinyl alcohol-d_2 obtained with thermal polarization and with signal enhancement provided by ODIP. Experiment is performed under PASADENA conditions at a sample temperature of 50 °C.

methylacrylate-d_2 due to the D–H coupling that leads to changes in the spectral pattern.

Styrene-d_2 contains a three-spin system of two deuterons and a proton, analogous to the case of methylacrylate-d_2. The signal enhancements provided by ODIP for this molecule are ε = 301 (D_A nucleus) and ε = 390 (D_B nucleus) (see Fig. 6). These values are almost two times lower than those for methylacrylate-d_2, most likely because of the lower reaction rate for phenylacetylene hydrogenation and faster quadrupolar relaxation of the D-nuclei in styrene-d_2.

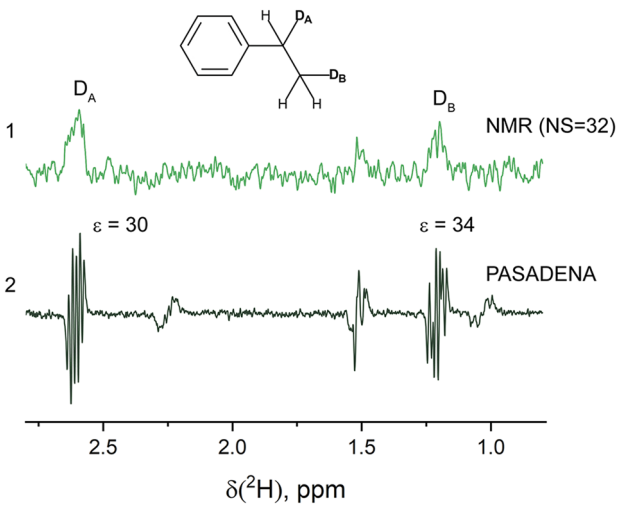

FIG. 8. ^{2}H NMR spectrum of ethylbenzene-d_2 obtained with thermal polarization and with signal enhancement provided by ODIP. Experiment is performed under PASADENA conditions at 50 °C.

The strongest ODIP-derived signal enhancements, ε = 682 for the D_A nucleus and ε = 1080 for the D_B nucleus, were obtained with vinyl alcohol-d_2, which is the smallest molecule used in our study (Fig. 7). The difference in the enhancement factors for the two coupled D-nuclei is most likely due to presence of additional splitting in the D_A multiplet, giving rise to the overlap of positive and negative NMR lines.

Finally, we have obtained moderate signal enhancements for ethylbenzene-d_2, which are about ε = 30 for the D_A nucleus and ε = 32 for the D_B nucleus (see Fig. 8). The ODIP spectrum of this compound is complex, which leads to significant line cancellation and, thus, to a reduced signal amplification. Another reason for low signal enhancement is fast polymerization of the styrene substrate at the elevated temperature of 50 °C. As a result, the compound with the longest T_1 among all the D-nuclei (Table I) considered in this study demonstrates the lowest enhancement. This is another indication of the fact that not only relaxation of D-nuclei but also the rate of the hydrogenation reaction plays an important role in the observed ODIP-derived signal amplification.

B. Spin order conversion in ODIP experiments

In addition to the standard PASADENA experiments, we have run experiments aimed at conversion of the initial anti-phase magnetization into in-phase magnetization. This goal is achieved by using out-of-phase echo detection (see Fig. 3).

The ODIP spectrum of methylacrylate-d_2 detected by using the out-of-phase echo sequences is presented in Fig. 9. One can see that the NMR signals of both D-nuclei change as compared to the PASADENA spectrum: the anti-phase signals are converted into pure in-phase signals demonstrating the validity of our experimental approach. This result is reproduced well by numerical simulations. Hence, the out-of-phase echo is indeed a suitable approach for spin order conversion, which allows one to avoid cancellation of positive and negative signals in ODIP spectra. The resulting enhancement factor for methylacrylate-d_2 in the out-of-phase echo experiment is equal to 490 for nucleus D_A and 470 for nucleus D_B. This result is the opposite of the PASADENA case where the D_A nucleus shows a smaller enhancement compared to D_B due to the stronger line cancellation in the antiphase multiplet. Refocusing of spin magnetization via the spin echo block eliminates line cancellation but leads to a polarization loss induced by T_2 relaxation, which is faster for the D_B nucleus (we assume that the fast motional regime is valid for the D-nuclei, and hence, $T_1 \approx T_2$; see Table I for the relaxation times). As a result, the signal enhancement in the out-of-phase echo experiment is smaller for the D_B nucleus than for the D_A nucleus; for both nuclei, the enhancement factor is lower than that observed in the PASADENA experiment. However, such a particular type of NMR experiment retains the potential of observing ODIP even when the external field is inhomogeneous, and the antiphase lines strongly cancel each other.

In order to optimize the performance of the spin echo sequence, we measured the signal intensity as a function of the inter-pulse delay τ_1. The resulting dependence was fitted by the following function:

$$\hat{I}_x(2\tau_1) \propto \sin(4\pi J\tau_1)\exp\left(-\frac{\tau_1}{T_2}\right) \quad (13)$$

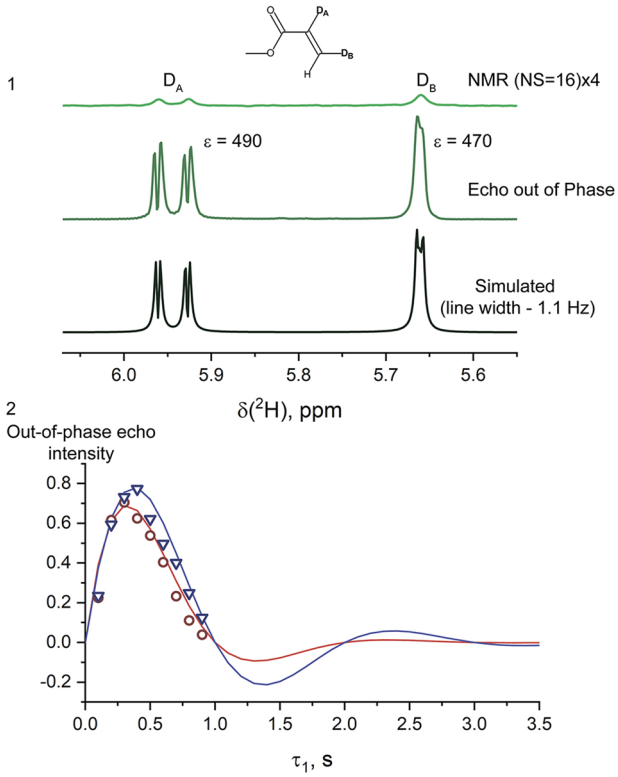

FIG. 9. Subplot 1: NMR spectrum detected with 16 acquisitions and multiplied by 4 (top), ODIP spectrum of methylacrylate-d_2 obtained by a single scan using the out-of-phase echo sequence (middle) and simulated out-of-phase echo spectrum with a linewidth of 1.1.Hz (bottom). Subplot 2: Dependence of the NMR line intensity on the inter-pulse delay τ_1 of the spin echo sequence (triangles for D_A, circles for D_B); solid lines show the modeling result. Scaling constant is the NMR line intensity in the PASADENA experiment under the same experimental conditions.

with sine modulation of the signal, as predicted by Eq. (12), and transverse relaxation with the characteristic time constant T_2, as shown in Fig. 9 yielding $T_2 = 0.5$ s. One can see that for such a short T_2, the oscillations in the τ_1-dependence due to J-coupling are strongly damped and only half of the first oscillation is clearly visible.

C. ODIP experiments with magnetic field variation

With the aim to gain additional insight into the spin dynamics underlying ODIP experiments, we also obtained ODIP spectra with magnetic field variation, which are commonly termed ALTADENA experiments (cf. Fig. 3). In our case, however, one must be careful when using the term "ALTADENA," which implies adiabatic variation of the spin Hamiltonian during the magnetic field switch $B_{pol} \rightarrow B_0$. The adiabaticity condition is usually, but not always,[17] fulfilled in PHIP experiments run with protons, which have much stronger spin–spin couplings. In the present case, however, the J-couplings are much smaller (e.g., the vicinal coupling of two D-nuclei is about only 0.25 Hz). Consequently, adiabatic field variation for D-nuclei is unlikely when the field switching time τ_{tr} is kept $\tau_{tr} < T_1$.

To obtain a quantitative measure for the degree of adiabaticity, we performed experiments and supported them by numerical modeling. The simplest system for the assessment of the effect of field variation is ethylcinnamate-d_2, where the D-nuclei form a two-spin system, which was treated analytically in the theory section. By comparing the stick spectrum calculated for field switching taking place in a real experiment (Fig. 10) with the spectral patterns shown in Fig. 2 (calculation assuming perfectly adiabatic field variation), one can see some remarkable difference. Specifically, in the "experimental" stick spectrum detected with a $\frac{\pi}{4}$-pulse, the components of the NMR multiplets have different sign, which is not possible for adiabatic field switching. Hence, the adiabaticity condition is not precisely fulfilled in our experiments. Another possible reason for the spectral pattern being different from the ALTADENA spectrum is that the reaction does not stop completely before sample transfer but goes on even when the sample is already at high field. This leads to a situation where hyperpolarization is partially formed at low field (ALTADENA condition) and partially at high field (PASADENA condition), and the spectrum yields a superposition of "in-phase" and "anti-phase" lines.

Under ALTADENA conditions, we managed to reach enhancement factors in ethylcinnamate-d_2 equal to $\varepsilon = 55$ (D_A nucleus) and $\varepsilon = 52$ (D_B nucleus) when the spectrum was detected with a $\frac{\pi}{4}$-pulse

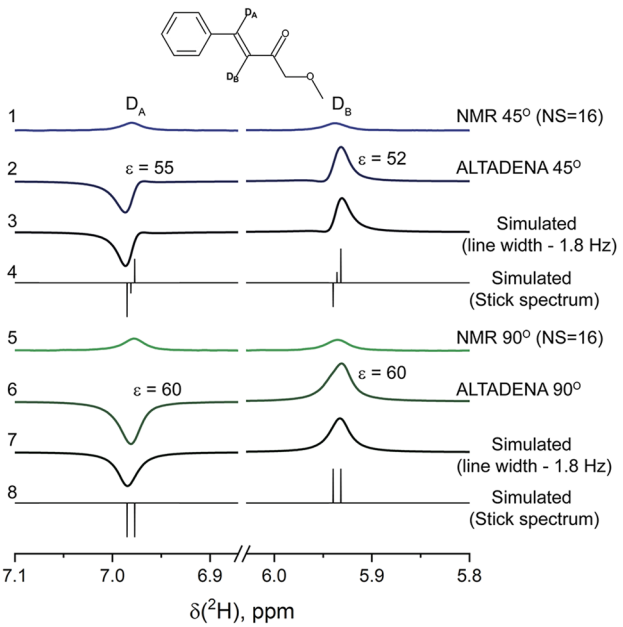

FIG. 10. ODIP spectrum of ethyl-cinnamate-d_2 obtained after the hydrogenation reaction performed at a low magnetic field. Here, we show for reference thermal spectra detected with $\frac{\pi}{4}$ (1) and $\frac{\pi}{2}$ (5) detection pulses, experimental ODIP spectra obtained with $\frac{\pi}{4}$ (2) and $\frac{\pi}{2}$ (6) detection pulses, and simulations of the experimental spectra presented with line broadening (3, 7) and as a stick spectrum (4, 8). The signal enhancement factors are indicated near the corresponding lines in the ALTADENA spectra. Sample temperature is 50 °C.

and $\varepsilon = 60$ (D_A nucleus) and $\varepsilon = 60$ (D_B nucleus) when the spectrum was detected with a $\frac{\pi}{2}$-pulse.

For methyl-acrylate-d_2 (three spin system of two ^{2}H nuclei and one proton), we observe an additional proton–deuteron multiplet effect (see Fig. 11). Such multiplet polarization is formed because at the preparation field the two ^{2}H-nuclei are strongly coupled and have unequal coupling to the third spin. Although generation of net polarization of the third spin is not possible in this case (the proton and deuterons are coupled only weakly), formation of the proton–deuteron multiplet spin order is allowed. This effect is known for PHIP[25] and has been described in detail in previous publications.[19,22] The ALTADENA enhancements for methyl-acrylate-d_2 are $\varepsilon = 1250$ (D_A nucleus) and $\varepsilon = 420$ (D_B nucleus) when the spectrum is detected with a $\frac{\pi}{4}$-pulse and $\varepsilon = 1350$ (D_A nucleus) and $\varepsilon = 44$ (D_B nucleus) when the spectrum is detected with a $\frac{\pi}{2}$-pulse.

All experimental spectra are in good agreement with the simulation.

D. ODIP PH-INEPT experiments

Transfer of PHIP is a common way of storing proton hyperpolarization by exploiting magnetic heteronuclei with long relaxation times, e.g., ^{13}C, ^{15}N, and others. In the case of deuterium, fast relaxation removes the non-equilibrium spin order on a timescale of a few seconds, rendering storage of ODIP-derived hyperpolarization problematic. For this reason, we have examined the possibility of transferring ODIP to heteronuclei, namely, ^{13}C nuclei, at the high magnetic field of the NMR spectrometer. A possible benefit of utilizing ODIP for transfer is that carbon nuclei in the deuterated product can have longer T_1 than in the same protonated product, which is the result of the smaller carbon–deuterium dipolar coupling.

For such a polarization transfer experiment, we have chosen methylpropiolate as a substrate because of the high enhancements obtained with this molecule in the PASADENA and ALTADENA experiments. The PH-INEPT [parahydrogen-INEPT (Insensitive Nuclei Enhancement by Polarization Transfer)] pulse sequence[24] was chosen to perform polarization transfer, since it is applicable to the case of spin order transfer from chemically inequivalent nuclei at high fields. Moreover, this method allows one to transfer polarization relatively fast, which is crucial in the case of D-nuclei. All experiments were performed at natural abundance of the carbon isotopes: since the amount of the ^{13}C isotopes is low (1.1% of ^{13}C), it is safe to assume that in each molecule, there is only one or no ^{13}C nuclei present. Hence, different signals in the ^{13}C spectrum correspond to different isotopomers, each having a single ^{13}C nucleus.

In our experiments, the INEPT pulses were applied on the ^{2}H and ^{13}C RF channels, leaving the proton spins unaffected. As a result, for calculating optimal INEPT delays, we restrict the simulation to a three-spin system (two ^{2}H spins and a single ^{13}C spin) introducing a single J_{D-D} coupling and two J_{D-C} couplings. We have performed OIDP transfer using three values of the τ_1 delay in the PH-INEPT sequence, which allowed us to reach a maximal enhancement of 300 for the ^{13}C nuclei (see Fig. 12). Variation in the delay

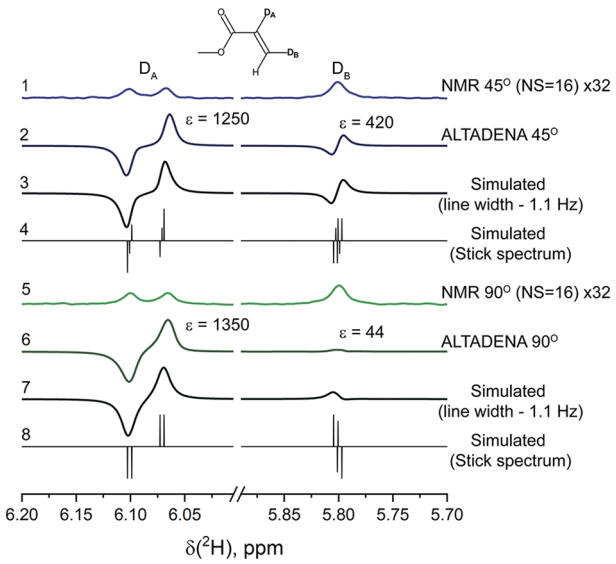

FIG. 11. ODIP spectrum of methyl-acrylate-d_2 obtained after the hydrogenation reaction performed at a low magnetic field. We show for reference thermal spectra detected with $\frac{\pi}{4}$ (1) and $\frac{\pi}{2}$ (5) detection pulses, experimental ODIP spectra obtained with $\frac{\pi}{4}$ (2) and $\frac{\pi}{2}$ (6) detection pulses, and simulation of the experimental spectra presented with line broadening (3, 7) and as a stick spectrum (4, 8). The signal enhancement factors are indicated near the corresponding lines in ALTADENA spectra. Sample temperature is 50 °C.

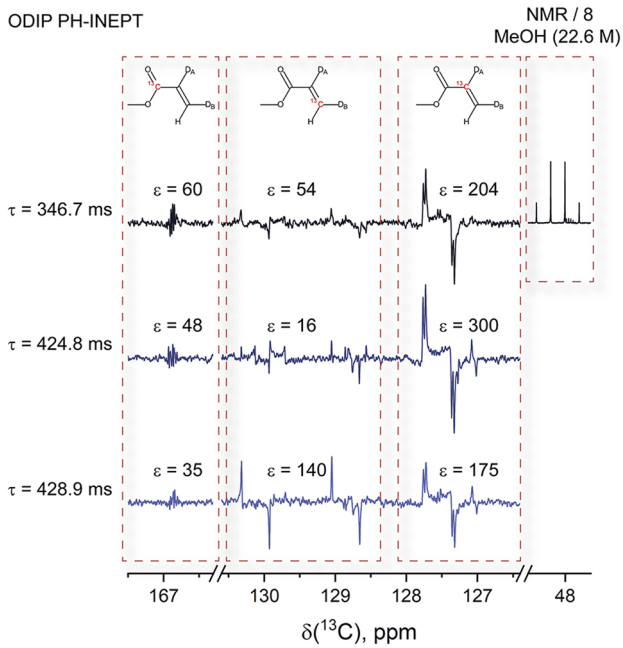

FIG. 12. ODIP spectrum of ^{13}C nuclei of methyl-acrylate-d_2 obtained using the PH-INEPT sequence with three different τ_1 delays. The signal enhancement factors are indicated for the corresponding lines in the ^{13}C ODIP PH-INEPT spectra. The concentration of the substrate molecules, which contribute to the hyperpolarized signal is 20 mM. The thermal NMR spectrum of the solvent (MeOH with 22.6M concentration) is presented as a reference.

τ_1 leads to different enhancements for the three isotopomers of the methylacrylate-d_2 molecule. The resulting signals are antiphase signals due to the anti-phase carbon–deuteron spin order, which are additionally split by the protons present in the molecule. Refocusing of these anti-phase signals into in-phase signals, e.g., using the PH-INEPT + sequence,[24] would potentially lead to a simpler spectral pattern, but the time required for the antiphase to in-phase conversion would require additional time. T_2 relaxation during the conversion period would then kick in, significantly reducing the achievable polarization gain.

IV. CONCLUSIONS

In this work, we have performed a systematic study of the spin dynamics underlying ODIP experiments. With the aim to develop quantitative description of ODIP, we have obtained analytical results for the ODIP nutation patterns under PASADENA and ALTADENA experimental conditions. When running experiments, we encountered difficulties with implementing ODIP. One of the problems comes from the small values of D–D scalar couplings and hence small splitting of the NMR lines: because of this, positive and negative lines partially cancel each other in our spectra. Also, the hydrogenation rates with D_2 appeared to be slower as compared to the case of H_2. To increase the reaction rates, we bubbled the D_2-gas through the solvent under elevated pressure and heated the sample up to 50 °C. Fast spin relaxation also necessitated optimization of the optimal bubbling time and delay between the bubbling period and NMR detection.

By using such an optimization for the PASADENA experiment, we have obtained sizable enhancement of the ^{2}H NMR signals for all substrates under study and achieved high reproducibility of the experiments. The signal enhancement factors are reaching approximately 1000. The spectral patterns agree well with simulation results for two-spin, three-spin, and five-spin systems. We have successfully exploited the out-of-phase echo pulse sequence. This method enables conversion of the anti-phase polarization into in-phase polarization, which is more suitable to NMR detection. We have run ALTADENA experiments for two substrates (methyl-propiolate and ethyl-phenyl-propiolate). A sample temperature of 50 °C was optimal for high signal enhancements. The shape of the spectra indicates that the adiabaticity condition for the field variation step is not fulfilled. Last but not least, we have demonstrated transfer of ODIP to heteronuclei, here, to ^{13}C nuclei.

Our results allow us to make some conclusions on the potential of the ODIP method. Despite the difficulties in running such experiments, this technique is feasible, and by proper optimization, NMR signal enhancements of the order of 1000 are possible, resulting in the largest ^{2}H hyperpolarization in liquids obtained so far. Potentially, comparison of PHIP and ODIP allows one also to obtain information about hydrogenation reactions and kinetic isotope effects therein.

ACKNOWLEDGMENTS

This work was supported by the Russian Fund for Basic Research (Grant No. 19-29-10028) in the theoretical study and by the Russian Science Foundation (Project No. 20-63-46034) in the experimental work. G.B. and S.K. acknowledge financial support by the DFG under Contract No. Bu-911-29-1. We acknowledge the Ministry of Science and Education of RF for providing access to NMR facilities at ITC.

APPENDIX A: SPIN STATES OF D_2 AND OPERATOR BASIS

The nuclear spin states of D_2 are as follows: The quintet states are

$$|Q_2\rangle = |\alpha\alpha\rangle, \quad |Q_1\rangle = \frac{1}{\sqrt{2}}(|\alpha\beta\rangle + |\beta\alpha\rangle),$$
$$|Q_0\rangle = \frac{1}{\sqrt{6}}(|\alpha\gamma\rangle + 2|\beta\beta\rangle + |\gamma\alpha\rangle), \tag{A1}$$
$$|Q_{-1}\rangle = \frac{1}{\sqrt{2}}(|\beta\gamma\rangle + |\gamma\beta\rangle), |Q_{-2}\rangle = |\beta\beta\rangle.$$

The triplet states are

$$|T_1\rangle = \frac{1}{\sqrt{2}}(|\alpha\beta\rangle - |\beta\alpha\rangle), \quad |T_0\rangle = \frac{1}{\sqrt{2}}(|\alpha\gamma\rangle - |\gamma\alpha\rangle),$$
$$|T_{-1}\rangle = \frac{1}{\sqrt{2}}(|\beta\gamma\rangle - |\gamma\beta\rangle). \tag{A2}$$

Finally, the singlet state is

$$|S\rangle = \frac{1}{\sqrt{3}}(|\alpha\gamma\rangle - |\beta\beta\rangle + |\gamma\alpha\rangle). \tag{A3}$$

Here, we introduce the states of spin-1 with the value of its z-projection,

$$|\alpha\rangle = |1,+1\rangle, \quad |\beta\rangle = |1,0\rangle, \quad |\gamma\rangle = |1,-1\rangle. \tag{A4}$$

The basis operators used to compose the density matrix of oD_2 are as follows:

$$\hat{I}_x = \frac{1}{\sqrt{2}}\left(\hat{T}_{1-1} - \hat{T}_{11}\right), \quad \hat{I}_y = \frac{i}{\sqrt{2}}\left(\hat{T}_{1-1} + \hat{T}_{11}\right), \quad \hat{I}_z = \hat{T}_{10},$$
$$\hat{I}_a = \sqrt{2}\hat{T}_{20} = \frac{1}{\sqrt{3}}\left(3\hat{I}_z^3 - 2\hat{E}\right), \quad \hat{I}_b = \frac{1}{\sqrt{2}}\left(\hat{T}_{2-1} - \hat{T}_{21}\right) = \left[\hat{I}_x, \hat{I}_z\right]_+. \tag{A5}$$
$$\hat{I}_c = \frac{-i}{\sqrt{2}}\left(\hat{T}_{2-1} + \hat{T}_{21}\right) = \left[\hat{I}_y, \hat{I}_z\right]_+, \quad \hat{I}_d = i\left(\hat{T}_{2-2} + \hat{T}_{22}\right) = \left[\hat{I}_x, \hat{I}_y\right]_+,$$
$$\hat{I}_e = \hat{T}_{2-2} + \hat{T}_{22} = \hat{I}_x^2 - \hat{I}_y^2$$

Here, $\hat{T}_{JM}$ are the components of irreducible spherical tensors[15] and $[\cdots,\cdots]_+$ stands for the anti-commutator of two operators.

APPENDIX B: SPIN STATES CORRELATION IN ALTADENA EXPERIMENT

A conventional ALTADENA experiment considers hydrogenation performed at the Earth magnetic field with subsequent adiabatic transport of the sample to the high NMR detection field. In this case, variation in the external magnetic field is supposed to be slow enough, thus the populations can follow the spin states changing

with time. Thus, correlation of low field and high field eigenstates allows one to predict the appearance of the hyperpolarized NMR spectrum. At the Earth magnetic field (order of several mT), the J-coupling value between two D-nuclei by far exceeds the difference of their Zeeman interactions with the field. Therefore, spin states with specific values of the total spin and its z-projection $|J, M_J\rangle$, i.e., quintet $|Q_M\rangle$, triplet $|T_M\rangle$, and singlet $|S\rangle$ states (Appendix A), are the eigenstates of the system. In the ODIP case, quintet and singlet states have non-equilibrium population in the course of chemical reaction at the low field. For a positive J-coupling value, correlation of these states with the high-field eigenstates demonstrates that the states $|\alpha\alpha\rangle$, $|\beta\alpha\rangle$, $|\alpha\gamma\rangle$, $|\gamma\alpha\rangle$, $|\gamma\beta\rangle$, and $|\gamma\gamma\rangle$ will be overpopulated after field variation [Fig. 13(1)]. This results in the continuous-wave NMR spectrum, and there will be two signals of opposite sign [see Fig. 13(2)] (as follows from the discussion in Sec. II A, consideration of Fourier NMR spectra is more complex, requiring analysis of the flip angle dependence). Inversion of the J sign changes the ordering of low-field eigenstates; as a result, the states $|\alpha\alpha\rangle$, $|\alpha\beta\rangle$ $|\alpha\gamma\rangle$, $|\gamma\alpha\rangle$, $|\beta\gamma\rangle$, and $|\gamma\gamma\rangle$ become over-populated [Fig. 13(3)], resulting in a sign change of the NMR pattern, as compared to the case $J > 0$ [Fig. 13(4)]. Considering the entire density matrix of the system, we can observe the sign change for the operators $\hat{I}_{1z}$, $\hat{I}_{2z}$ (representing net magnetization) and for the operators $\hat{I}_{1a}\hat{I}_{2z}$, $\hat{I}_{1z}\hat{I}_{2a}$ (which stand for three-spin order) present in the density matrix given by Eq. (10), whereas the contributions from two-spin order remain the same. Thus, the resulting density matrix of the two D-nuclei in the ALTADENA case with negative J-value becomes

$$\hat{\rho}_A = \frac{2}{3}\hat{E} + \frac{1}{6}\left[-\hat{I}_{1z} + \hat{I}_{2z} - \sqrt{3}\left(\hat{I}_{1a}\hat{I}_{2z} - \hat{I}_{1z}\hat{I}_{2a}\right) + \sqrt{3}\left(\hat{I}_{1a} + \hat{I}_{2a}\right)\right]. \quad \text{(B1)}$$

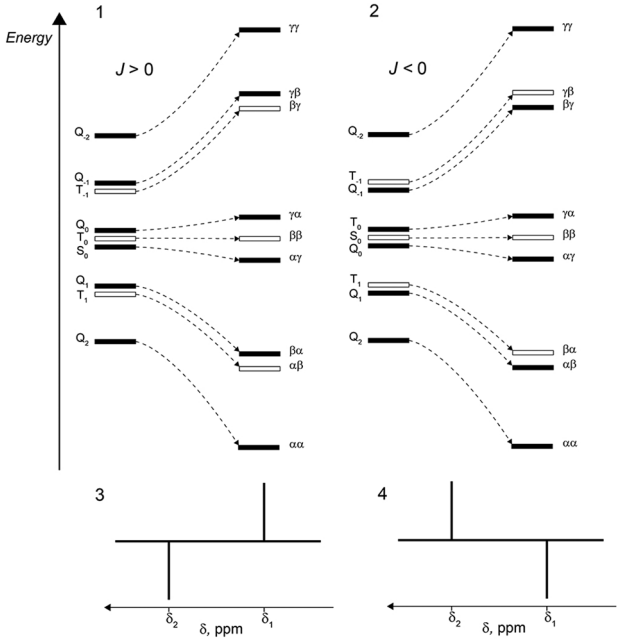

FIG. 13. Correlation diagram for spin states in the ALTADENA experiment in the case of a positive J-value (1) and the corresponding continuous-wave NMR spectrum (3). Correlation diagram for spin states in the ALTADENA experiment in the case of negative J-value (2) and the corresponding continuous-wave NMR spectrum (4). Black rectangles indicate spin states with ODIP-derived populations (plotted assuming 100% enrichment of the *ortho*-states). In the correlation diagrams, the low-field states are plotted at the left, whereas the high-field states are plotted at the right.

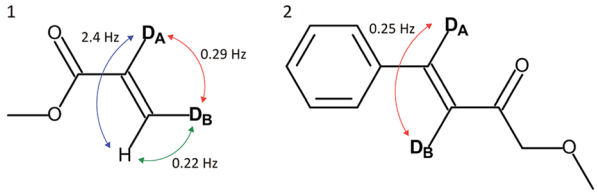

FIG. 14. Spin–spin coupling values in methylacrylate-d_2 (1) and ethylcinnamate-d_2 (2).

APPENDIX C: NMR PARAMETERS FOR USED MOLECULES

As discussed in the main text of this paper, one of the major difficulties when working with ODIP is given by the small values of typical ^{2}H spin–spin couplings. The gyromagnetic ratio for ^{2}H nuclei is 6.5 times smaller than that for protons. Hence, all deuteron–proton couplings are equal to the corresponding proton–proton couplings divided by 6.5. To calculate deuteron–deuteron coupling, one may divide the corresponding proton–proton coupling by $(6.5)^2 = 42.25$. Typical J-coupling values for methylacrylate-d_2 and ethylcinnamate-d_2 are presented on Fig. 14. Approximation of these values was made by dividing the couplings in the corresponding protonated molecules by numeric factors of 6.5 (for the proton–deuteron couplings) and 42.25 (for the deuteron–deuteron couplings). Numerical calculation of PASADENA spectra allowed us to adjust these values by comparing simulated and experimental ODIP spectra.

DATA AVAILABILITY

The data that support the findings of this study are available from the corresponding author upon reasonable request.

REFERENCES

[1]C. R. Bowers and D. P. Weitekamp, Phys. Rev. Lett. **57**, 2645 (1986).
[2]J. Natterer and J. Bargon, Prog. Nucl. Magn. Reson. Spectrosc. **31**, 293 (1997).
[3]R. A. Green, R. W. Adams, S. B. Duckett, R. E. Mewis, D. C. Williamson, and G. G. R. Green, Prog. Nucl. Magn. Reson. Spectrosc. **67**, 1 (2012).
[4]C. R. Bowers and D. P. Weitekamp, J. Am. Chem. Soc. **109**, 5541 (1987).
[5]S. B. Duckett and R. E. Mewis, Acc. Chem. Res. **45**, 1247 (2012).
[6]R. W. Adams, J. A. Aguilar, K. D. Atkinson, M. J. Cowley, P. I. P. Elliott, S. B. Duckett, G. G. R. Green, I. G. Khazal, J. López-Serrano, and D. C. Williamson, Science **323**, 1708 (2009).
[7]J. Natterer, T. Greve, and J. Bargon, Chem. Phys. Lett. **293**, 455 (1998).
[8]A. Limbacher, Ph.D. thesis, Mathematisch-Naturwissenschaftliche Fakultät, Rheinische Friedrich-Wilhelms-Universität Bonn, Bonn, 2004, p. 81.
[9]T. Jonischkeit, Ph.D. thesis, Mathematisch-Naturwissenschaftliche Fakultät, Rheinische Friedrich-Wilhelms-Universität Bonn, Bonn, 2004.

[10]A. Jhajharia, E. M. M. Weber, J. G. Kempf, D. Abergel, G. Bodenhausen, and D. Kurzbach, J. Chem. Phys. **146**, 041101 (2017).
[11]K. L. Ivanov, T. Kress, M. Baudin, D. Guarin, D. Abergel, G. Bodenhausen, and D. Kurzbach, J. Chem. Phys. **149**, 054202 (2018).
[12]D. Kurzbach, E. M. M. Weber, A. Jhajharia, S. F. Cousin, A. Sadet, S. Marhabaie, E. Canet, N. Birlirakis, J. Milani, S. Jannin, D. Eshchenko, A. Hassan, R. Melzi, S. Luetolf, M. Sacher, M. Rossire, J. Kempf, J. A. B. Lohman, M. Weller, G. Bodenhausen, and D. Abergel, J. Chem. Phys. **145**, 194203 (2016).
[13]S. Aime, R. Gobetto, F. Reineri, and D. Canet, J. Chem. Phys. **119**, 8890 (2003).
[14]M. G. Pravica and D. P. Weitekamp, Chem. Phys. Lett. **145**, 255 (1988).
[15]V. K. Khersonskii, A. N. Moskalev, and D. A. Varshalovich, *Quantum Theory of Angular Momemtum* (World Scientific, 1988).
[16]G. Buntkowsky and H.-H. Limbach, in *Hydrogen-Transfer Reactions* (Wiley-VCH Verlag GmbH & Co. KGaA, 2007), p. 639.
[17]S. E. Korchak, K. L. Ivanov, A. V. Yurkovskaya, and H.-M. Vieth, Phys. Chem. Chem. Phys. **11**, 11146 (2009).
[18]K. L. Ivanov, A. V. Yurkovskaya, and H.-M. Vieth, J. Chem. Phys. **128**, 154701 (2008).
[19]K. L. Ivanov, A. V. Yurkovskaya, and H.-M. Vieth, Z. Phys. Chem. **226**, 1315 (2012).
[20]S. Schäublin, A. Höhener, and R. R. Ernst, J. Magn. Reson. **13**, 196 (1974).
[21]A. N. Pravdivtsev, K. L. Ivanov, A. V. Yurkovskaya, H.-M. Vieth, and R. Z. Sagdeev, Dokl. Phys. Chem. **465**, 267 (2015).
[22]A. S. Kiryutin, K. L. Ivanov, A. V. Yurkovskaya, R. Kaptein, and H.-M. Vieth, Z. Phys. Chem. **226**, 1343 (2012).
[23]A. S. Kiryutin, G. Sauer, S. Hadjiali, A. V. Yurkovskaya, H. Breitzke, and G. Buntkowsky, J. Magn. Reson. **285**, 26 (2017).
[24]M. Haake, J. Natterer, and J. Bargon, J. Am. Chem. Soc. **118**, 8688 (1996).
[25]S. Aime, R. Gobetto, F. Reineri, and D. Canet, J. Magn. Reson. **178**, 184 (2006).